J Chem Crystallogr (2010) 40:753–760
DOI 10.1007/s10870-010-9732-8

ORIGINAL PAPER

On the Two Closely Related Phases of [Ru(C_5Me_5)(η^6-1,3-(Me_2NCH_2)$_2C_6H_4$)](BF_4) and the Reversible Solid–Solid Order–Disorder Phase Transition

Maxime A. Siegler · Sylvestre Bonnet · Antoine M. M. Schreurs · Robertus J. M. Klein Gebbink · Gerard van Koten · Anthony L. Spek

Received: 15 April 2008 / Accepted: 11 February 2010 / Published online: 3 March 2010

Abstract Crystals of the complex [Ru(C_5Me_5)(η^6-1,3-(Me_2NCH_2)$_2C_6H_4$)](BF_4) have been examined over the temperature range 150–300 K via X-ray diffraction measurements. This study shows that the Ru complex is a two-phase system in this *T*-range and the solid–solid transition is reversible. At 150 K, phase II ($P2_1/c$, $Z' = 4$) is ordered and non-merohedrally twinned, $a = 16.4396$ (9) Å, $b = 17.3226$ (4) Å, $c = 32.1874$ (11) Å, $\beta = 91.375$ (2)°. At 295 K, phase I ($Pbca$, $Z' = 1$) is disordered, $a = 8.5071$ (3) Å, $b = 17.1567$ (3) Å, $c = 32.8250$ (8) Å. The relationship between the two phases is obvious because the packing remains similar in the two phases. The greatest structural changes between the two phases are found in the rows of adjacent cations [Ru(C_5Me_5)(η^6-1,3-(Me_2NCH_2)$_2C_6H_4$)]$^+$ packed along the **a** direction. These rows are ordered in phase II but are disordered in phase I. The phase transition is first order. Significant changes in thermal motion for the cations are considered as being the driving force for the occurrence of this phase transition.

Keywords Solid–solid phase transition · Polymorphism · First-order

Electronic supplementary material The online version of this article (doi:10.1007/s10870-010-9732-8) contains supplementary material, which is available to authorized users.

M. A. Siegler · A. M. M. Schreurs · A. L. Spek
Crystal and Structural Chemistry, Bijvoet Center for Biomolecular Research, Faculty of Science, Utrecht University, Padualaan 8, 3584 CH Utrecht, The Netherlands

S. Bonnet · R. J. M. Klein Gebbink · G. van Koten
Organic Synthesis and Catalysis, Debye Institute for Nanomaterials Science, Faculty of Science, Utrecht University, Padualaan 8, 3584 CH Utrecht, The Netherlands

M. A. Siegler (✉)
Department of Chemistry, The Johns Hopkins University, New Chemistry Building, Small Molecule X-Ray Crystallography Facility, Rooms 211 (Office) and 240 (X-Ray Lab), 3400N. Charles St., Baltimore, MD 21218, USA
e-mail: xray@jhu.edu; msiegle2@jhu.edu

S. Bonnet
Leiden Institute of Chemistry, Gorlaeus Laboratories, Leiden University, PO Box 9502, 2300 RA Leiden, The Netherlands

Introduction

NCN-pincer metal complexes with the general formula [MX(2,6-(Me_2NCH_2)$_2C_6H_3$)] (M = Pd, Pt and X = Cl, Br, I) have been studied extensively for three decades [1], notably for their ability to bind small molecules such as I_2 or SO_2 (M = Pt) [2], and for their catalytic properties (M = Pd) [3]. It was recently shown that η^6-coordination of a [Ru(C_5Me_5)]$^+$ fragment can take place selectively and efficiently at the central arene ring of NCN-pincer metal complexes without destabilization of the η^1 carbon-to-metal bond (Scheme 1) [4]. The obtained complexes are the η^6, η^1 heterobimetallic complexes $\mathbf{3}^+$–$\mathbf{4}^+$ built around the arene ring of the NCN-pincer ligand. In such complexes, the η^6-coordinated metal fragment has strong electron-withdrawing properties on the η^1-coordinated pincer metal center. Demetalation of the pincer metal complex may occur during η^6-coordination of the [Ru(C_5Me_5)]$^+$ fragment when the metal M is not Pt^{II} or Pd^{II} [Bonnet S, Siegler MA, Lutz M, Spek AL, van Koten G, Klein Gebbink RJM, "unpublished works"]. In order to confirm this, the monometallic analog [Ru(C_5Me_5)(η^6-1,3-(Me_2NCH_2)$_2C_6H_4$)](BF_4) {hereafter, [**6**](BF_4)}, in which the [MCl]$^+$ fragment is replaced by a proton, was synthesized.

Scheme 1 Syntheses of complexes $\mathbf{3}^+$, $\mathbf{4}^+$ and $\mathbf{6}^+$

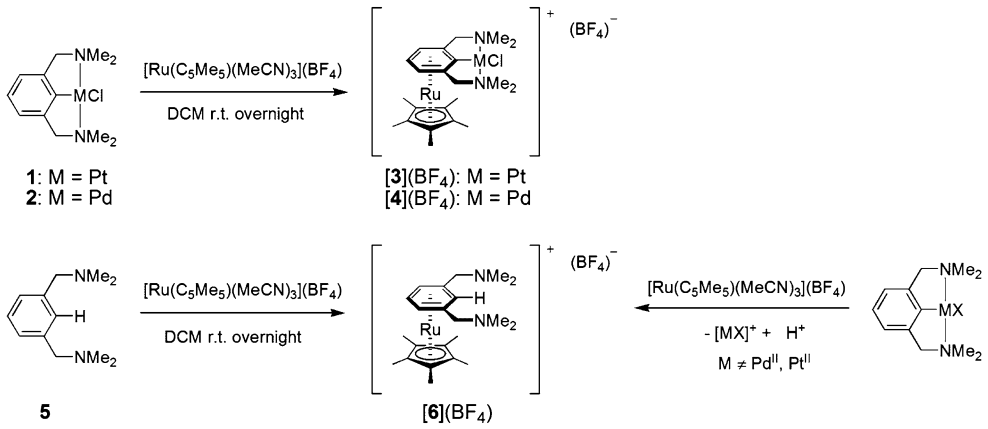

Examination of the monometallic complex [**6**](BF_4) was carried out via a series of X-ray diffraction measurements between 150 and 300 K. A first set of data was collected near 150 K and an ordered phase with $Z' = 4$ (i.e., phase II) was found. Inspection of the diffraction pattern for this high-Z' phase showed clear evidence of twinning. The structure of this phase was found to be pseudo-symmetric. In some compounds for which high-Z' structures are thermodynamically stable at low temperature, it has been observed that other phases with lower Z' may be found at higher temperature and are closely related to the low-temperature phases [5, 6]. Such systems exhibit polymorphism [7]. Another set of data was collected near room temperature, and a new disordered phase with $Z' = 1$ (i.e., phase I) was found. In this system, it is remarkable that no significant loss of crystallinity takes place as single crystals undergo the transition.

The X-ray structure determination analysis shows that the packing remains similar in the two phases, and that the greatest structural changes take place along the **a** direction. The investigation for finding the nature and the temperature of the phase transition was carried out by examining the temperature dependence of the cell dimensions, which had proved to be informative in other systems [8–10]. This study emphasizes that the solid–solid transition, which takes places between 212 and 218 K, is reversible and first-order.

Experimental

Synthesis

Compound $[Ru(C_5Me_5)(MeCN)_3](BF_4)$ [11] (58 mg, 129 μmol) was dissolved in dry, distilled dichloromethane (2.5 mL). The solution was cannulated under nitrogen onto 1,3-$(Me_2NCH_2)_2C_6H_4$ (36 mg, 181 μmol) and the mixture stirred under nitrogen for 16 h. Dichloromethane was removed under vacuum, and the crude product was purified on a 50 mL alumina column using a dichloromethane/methanol mixture (99:1 v/v) as eluent. The purified complex was reprecipitated from dichloromethane/pentane (32 mg, 48%).

^{1}H NMR (400 MHz, δ in acetone-d6): 6.05 (m, 4H, arom), 3.33 (d, 2H, CHN, J = 12.9 Hz), 3.29 (d, 2H, CH′N, J = 12.9 Hz), 2.26 (s, 12H, NMe_2), 2.00 (s, 15H, C_5Me_5). ^{13}C NMR (100 MHz, δ in acetone-d6): 100.6 ($C_4 + C_6$), 96.9 (C^{IV}(Cp*)), 90.7 (C_2), 89.5 ($C_1 + C_3$), 88.7 (C_5), 61.1 (CH_2N), 45.0 (NMe_2), 10.4 (Cp*). MALDI TOF m/z (calc): 429.11 (429.18, $[M\text{-}BF_4]^+$).

Crystal Growth

Pale blue crystals of [**6**](BF_4) were grown in a small vial at room temperature by slow vapor diffusion of pentane (i.e., counter-solvent) into dichloromethane and appeared after a few days. Most of the time, crystals were found to be very thin plates, but some thicker plates could be found on the inner walls of the vial.

X-ray Crystallography

All reflection intensities were measured using a Nonius KappaCCD diffractometer (rotating anode) with graphite-monochromated Mo $K\alpha$ radiation ($\lambda = 0.71073$ Å) under the program *COLLECT* [12]. The program PEAKREF [13] was used to determine the cell dimensions. Data reduction was done using the program *EVALCCD* [14] for phase I (i.e., the room-temperature phase) and the program *EVAL15* [15] (a data integration method using profile prediction) for phase II (i.e., the low-temperature phase). The latter program helped to integrate more accurately the weak and overlapping reflections of the twinned structure. The structure of phase I was solved with the program *DIRDIF99* [16] and the structure of phase II was solved with the program *SHELXS86* [17]. The two structures were refined on F^2 with *SHELXL97* [18]. Multi-scan semi-empirical absorption corrections were applied to the data of

phase I using the program *SADABS* [19]. Applying an absorption correction to the data of phase II using the program *TWINABS* [20] did not improve the least squares refinement (i.e., there was no significant improvement on the *R*-factor and on the residual electron density), subsequently the absorption correction was not retained. The temperature of the data collection was controlled using the system *OXFORD CRYOSTREAM 600* (manufactured by *OXFORD CRYOSYSTEMS*). The H-atoms were placed at calculated positions (*AFIX 23* or *AFIX 43* or *AFIX 137*) with isotropic displacement parameters having values 1.2 or 1.5 times U_{eq} of the attached C atom. The atom-numbering scheme was made consistent for the two phases (Fig. 1). For all sets of measurements, the same crystal was used since no significant loss of crystallinity occurs as the crystal was either cooled or heated.

Data for phase I (*Pbca*, $Z' = 1$) were collected at 295 K. The structure of this phase is very disordered. The refinement against F^2 was good: the *R* factor [$F^2 > 2\sigma(F^2)$] is slightly higher than 0.040 and the final difference Fourier map showed no peaks larger than 0.54 e $Å^{-3}$. The anisotropic displacement parameters (hereafter, ADPs) of all related disordered atoms were constrained to be identical (*EADP* instruction). Restraints were applied so that the minor and major components of the disordered cation and those of the disordered counter anion have similar geometries (*SADI* and *SAME* instructions). The *DELU* instruction (i.e., a rigid bond restraint) had to be applied to all atoms of the cation in order to get a satisfactory refinement. The values of the occupancy factors given for the major component of the disordered cation and that of the disordered counter anion refine to 0.680 (5) and 0.816 (5).

Data for phase II ($P2_1/c$, $Z' = 4$) were collected at 150 K after the crystal had been flash-cooled from room temperature (phase II could be also obtained if the crystal had been slowly cooled at −2 K/min from room temperature). This phase is ordered and is non-merohedrally twinned. In the process of determining the cell dimensions, the program *DIRAX* [21] found the twin relationship for which the two domains are related by a twofold axis along the **c** direction. In order to maximize the separation of the non-overlapping reflections, data were collected with a crystal-to-detector distance of 70 mm. Inspection of the reconstructed reciprocal lattice slices down the **b*** direction showed clear evidence of twinning (Fig. 2). The refinement against F^2 was fair for a twinned structure: the *R* factor [$F^2 > 2\sigma(F^2)$] is slightly higher than 0.075 and the final difference Fourier map showed peaks as large as 1.52 e $Å^{-3}$ (the largest peaks are always found to be close to all four independent Ru atoms). The fractional contribution of the minor twinned component refines to 0.364 (4). The ADPs were refined without any constraints for all independent non-H atoms. No geometry restraints were necessary for this refinement. The consistency of the bond distances for all independent cations (excluding hydrogen atoms) and anions was good; the estimated standard deviations for the sets of chemically equivalent distances averaged about 1.1 times the average uncertainty of an individual measurement.

The crystallographic data for the two phases of the compound [**6**](BF_4) are given in Table 1. The displacement ellipsoids of all atoms in the asymmetric units of phases I and II are shown in Fig. 3.

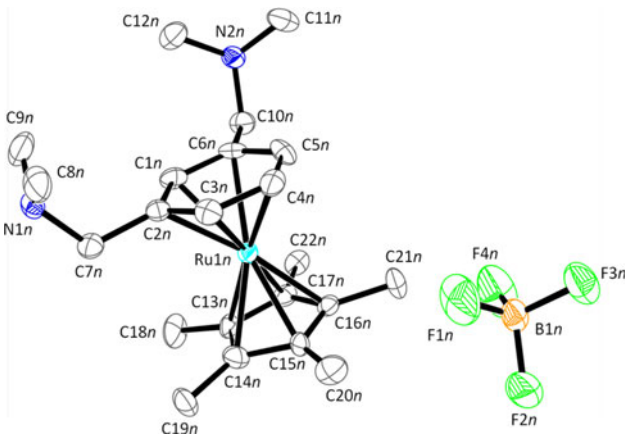

Fig. 1 Displacement ellipsoid plot (50% probability level) of one formula unit of [**6**](BF_4) in phase II at 150(1) K. The atomic numbering scheme is consistent for the four crystallographically independent formula units found in phase II and the disordered formula unit found in phase I. In phase II, *n* takes the values 1–4, respectively for the formula units 1–4

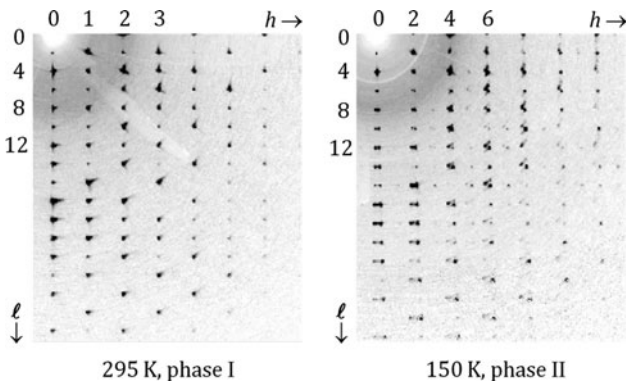

Fig. 2 Parts of the reciprocal lattice slices $h0\ell$ digitally reconstructed from the measured frames given for phase I (295 K) and for phase II (150 K). At room temperature, the reflections look normal (although streaks appear near the strongest reflections) and there is no sign of twinning. At 150 K, the splitting of the reflections at higher resolution is obvious and the crystal is non-merohedrally twinned (see text)

Table 1 Crystallographic data for the phases I and II of the complex [**6**](BF_4)

	I	II
Crystal data		
Chemical formula	$C_{22}H_{35}N_2Ru.BF_4$	$C_{22}H_{35}N_2Ru.BF_4$
M_r	515.40	515.40
Cell setting, space group	Orthorhombic, *Pbca*	Monoclinic, $P2_1/c$
Temperature (K)	295 (2)	150 (1)
a, b, c (Å)	8.5071 (3), 17.1567 (3), 32.8250 (8)	16.4396 (9), 17.3226 (4), 32.1874 (11)
β (°)	–	91.375 (2)
V (Å^3)	4790.9 (2)	9163.6 (6)
Z; Z'	8; 1	16; 4
D_x (Mg m^{-3})	1.429	1.494
Radiation type	Mo $K\alpha$	Mo $K\alpha$
No. of reflections for cell parameters	9476	3863
θ range (°)	2.37–27.43	2.43–27.47
μ (mm^{-1})	0.70	0.73
Crystal form, colour	Plate, light blue	Plate, light blue
Crystal size (mm)	0.20 × 0.15 × 0.11	0.20 × 0.15 × 0.11
Data collection		
Data collection method	ϕ and ω scans	ϕ and ω scans
Absorption correction	Multi-scan (based on symmetry-related measurements)	None
T_{min}	0.683	–
T_{max}	0.921	–
No. of measured, independent and observed reflections	37942, 4465, 3007	16075, 16075, 10368
Criterion for observed reflections	$I > 2\sigma(I)$	$I > 2\sigma(I)$
R_{int}	0.063	0.196
θ_{max} (°)	25.5	25.0
Refinement		
Refinement on	F^2	F^2
$R[F^2 > 2\ \sigma(F^2)]$, $wR(F^2)$, S	0.041, 0.113, 1.05	0.076, 0.189, 1.13
No. of reflections	4465	16075
No. of parameters	381	1118
Weighting scheme	Calculated $w = 1/[\sigma^2(F_o^2) + (0.0467P)^2 + 6.1732P]$ where $P = (F_o^2 + 2F_c^2)/3$	Calculated $w = 1/[\sigma^2(F_o^2) + (0.0184P)^2 + 61.8765P]$ where $P = (F_o^2 + 2F_c^2)/3$
$(\Delta/\sigma)_{max}$	0.001	0.001
$\Delta\rho_{max}$, $\Delta\rho_{min}$ (e Å^{-3})	0.54, −0.34	1.50, −0.86

Temperature Dependence of the Cell Dimensions

Two sets of data using an automatic procedure based on the phi/chi cell determination method [22] were collected in order to derive the temperature dependence of the cell dimensions for the polymorphic system [**6**](BF_4) in both cooling and heating regimens (Figs. S1, S2). All reflection intensities (i.e., near 800 reflections) were measured in the T-ranges 150–300 K at ±10 K intervals (data set 1) and in 200–230 K at ±3 K intervals (data set 2) using a Nonius KappaCCD diffractometer equipped with a fine-focus sealed tube. The cooling/heating rates were set to ±2 K/min. The crystal to detector distance was fixed at 70 mm throughout the whole series of measurements. The V/Z (volume per formula unit) versus T plot reported for the second data set is shown in Fig. 4.

Results and Discussion

Generalities

Ruthenation of the free NCN-pincer ligand 1,3-$(Me_2NCH_2)_2C_6H_4$ afforded complex [**6**](BF_4) in moderate

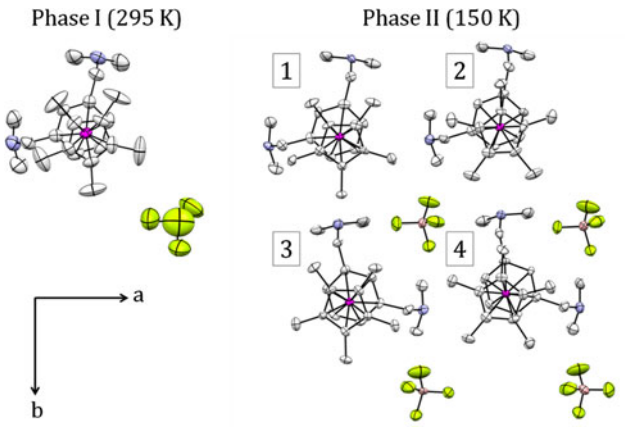

Fig. 3 Displacement ellipsoid plots (50% probability level) of the asymmetric units of [**6**](BF_4) in phase I at 295(2) K and in phase II at 150(1) K. The four crystallographically independent formula units found in the asymmetric unit of phase II are numbered 1–4. H atoms and disorder (phase I) are omitted for the sake of clarity

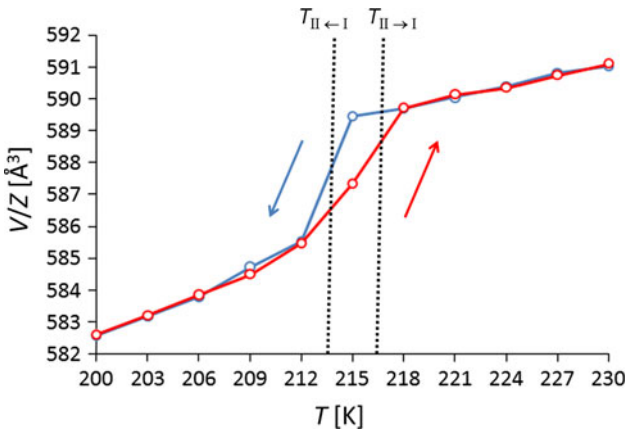

Fig. 4 Plot of the volume per formula unit V/Z (Å^3) versus T (K). Values of V/Z are measured for the solid–solid phase transition I ↔ II (T-range: 200–230 K) at ±2 K for both cooling (*blue lines*) and heating (*red lines*) regimens. The positions of the vertical thin lines give the estimated temperatures for which the discontinuities occur. Error bars associated with V/Z are not reported since they are insignificant compared to the y-axis scale. (Color figure online)

yield due to the presence of the free amine arms (Scheme 1). The ^{1}H and ^{13}C NMR spectra are consistent with η^6-coordination of the $[Ru(C_5Me_5)]^+$ fragment to the aromatic ring of the ligand. The aromatic signals are indeed shifted to much higher fields compared to the free ligand [11], and the benzylic protons give an AB system instead of a singlet, without any appreciable change in chemical shift compared to the free ligand.

Cation Geometries

In the structures of phases I and II, the arene and the pentamethylcyclopentadienyl aromatic ligand (hereafter, Cp*) of the cation $\mathbf{6}^+$ are, respectively η^6- and η^5-bonded to the Ru(II) metal center, allowing the two nitrogen atoms to remain non-coordinated. Unlike in $[\mathbf{3}]^+$ and $[\mathbf{4}]^+$ [4], where the nitrogen atoms are coordinated to the pincer metal (and hence geometrically constrained), the non-coordinated amine 'arms' are free to rotate around the C–C and C–N single bonds in $[\mathbf{6}]^+$. In the molecular structure of [**6**]BF_4, these 'arms' accommodate the steric hindrance of the bulky Cp* ligand by sitting opposite to it with respect to the benzylic carbon atoms. The molecular planes of the two carbocycles are nearly parallel with each other, and nearly perpendicular to the coordination axis [i.e., the axis defined by the centroids Cg(arene) and Cg(Cp*)]: the Cg(arene)–Ru–Cg(Cp*) angles are almost 180° for cations found in both phases. The distances between the Ru atom and the averages planes of the arene and Cp* rings are very similar in the four crystallographically independent cations of phase II: the average Ru–Cg(arene) and Ru–Cg(Cp*) distances are about 1.699(2) and 1.814(4) Å, respectively. In phase I, the Ru–Cg(arene) distance remains very similar but the Ru–Cg(Cp*) is slightly longer [$\sim$1.857(6) Å].

In the structure of phase II, half of the four independent cations differ in conformation since the Cp* ligands may adopt two different orientations. All four cations have a pseudomirror plane nearly perpendicular to the arene ring (passing through the C1 and C4 atoms).

In the structure of phase I, the difference in conformation is still noticeable but the cation is wholly disordered. Overall, the cation geometry remain very similar in the two phases.

The lone pairs of the nitrogen atoms (except for one nitrogen atom of the minor component of the disordered cation in phase I) point outwards the cations, so that weak C(arene)–H···N interactions [d(H···N) $\sim$ 2.7 Å on average] take place between two adjacent cations along the **b** direction. Such contacts are more difficult to observe in phase I because of the disorder.

Table 2 includes selected distances and angles for the phases I and II of [**6**](BF_4).

Crystal Packing

In the two phases of [**6**](BF_4), the cations and counter anions form two-dimensional (hereafter, 2-D) planes parallel to (0 0 1) (Fig. 5). These planes, along which the counterions are encapsulated in 'pockets' formed by four neighbouring cations, are stabilized by weak cation···anion interactions C–H···F ranging between 2.4 and 2.7 Å. The largest structural changes between the structures of phases I and II are found along the **a** direction. In phase II, two successive independent cations along the **a** direction differ in conformation since the Cp* ligands adopt two different orientations. Rows of adjacent cations along this direction are ordered in phase II. Phase I may be described as the

Table 2 Selected bond distances (Å) and bond angles (°) for the four independent cations described in phase II and for the major component of the disordered cation described in phase I

	I	II			
		1	2	3	4
Ru–Cg(arene)	1.705 (5)	1.701 (3)	1.696 (3)	1.701 (3)	1.698 (3)
Ru–Cg(Cp*) (Å)	1.857 (6)	1.811 (3)	1.815 (4)	1.810 (3)	1.819 (3)
Cg(arene)–Ru–Cg(Cp*)	178.8 (3)	179.40 (17)	179.37 (18)	178.97 (17)	179.39 (17)

average structure of phase II, for which adjacent cations are related by an approximate translation of $a_{II}/2$ and are crystallographically equivalent; this requires the cations to be disordered.

Relationship Between Phases I and II

The relationship between phases I and II is obvious since the packing remains similar in both phases. The transformation matrix **M** that relates the unit cells of phase I and II can be approximated by **M** ≈ (2 0 0 / 0 1 0 / 0 0 1) (this transformation matrix remains an approximation because the β angle for phase II is close enough to 90°).

Pseudosymmetry in Phase II

In the structure of phase II, the four crystallographically independent formula units numbered 1–4 (see Fig. 3 for numbering) can be related by pseudo-glide plane and pseudo-translation symmetries.

The cations 1 and 3 (as well as the cations 2 and 4) are related by a pseudo-glide plane nearly perpendicular to the *a* axis with a translation of *b*/2. The distances Ru11···Ru13 and Ru12···Ru14 are found to be 8.6378 (11) and 8.6900 (11) Å, which are about 0.3% shorter and 0.3% longer than *b*/2 [8.6613 (4) Å]. A quaternion fit [23] of the cation 1 (Ru11) with the cation 3 (Ru13) was made via the program *PLATON—AutoMolFit* [24] and confirmed that the two cations are related by a pseudo *b* glide plane almost perpendicular to the *a* axis (Fig. 6a). The calculated lattice vector that relates both cations is given by [0.016 1.000 0.003] with a shift of 8.634 Å (i.e., approximately *b*/2). The overall root-mean square (hereafter, rms) deviation for fitting is only 0.06 Å (excluding the hydrogen atoms and the counter anions), which is very good. The same method for fitting the cations 2 and 4 gives very similar results: a lattice vector of [−0.017 1.000 −0.003] with a shift of 8.670 Å and the rms deviation is also 0.06 Å (excluding the hydrogen atoms and the counter anions). An inspection of the reciprocal lattice slice 0*k* ℓ showed that the *k* odd reflections are nearly absent, which also suggests the existence of a pseudo *b* glide plane perpendicular to *a*.

The formula units 1 and 2 (as well as 3 and 4) are related by a pseudo-translation of *a*/2. The distances Ru11···Ru12

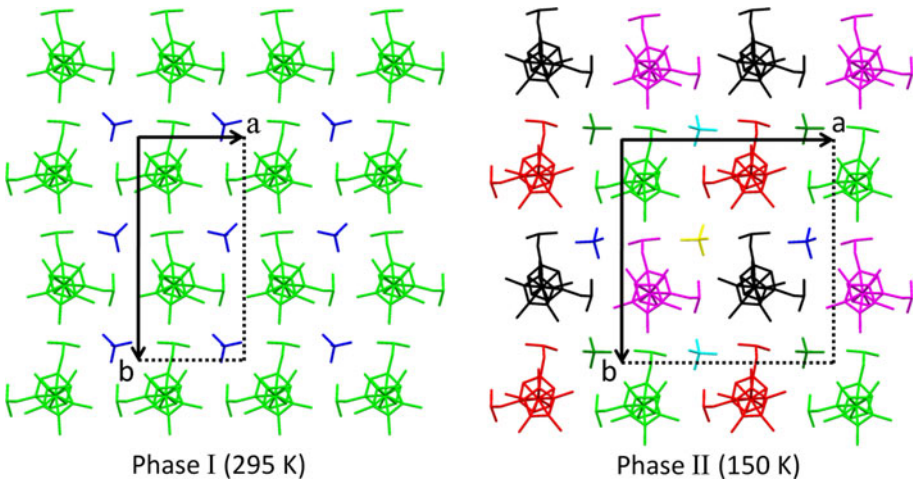

Fig. 5 The packing of one layer of [**6**](BF$_4$) in the phases I and II looking down the **c** direction. For phase II, the *a* axis is not in the plane of the drawing. The cations and counter anions form 2-D planes parallel to (0 0 1). The drawing shows that the packing is similar in the two phases although the orientations of the counter anions may vary. In phase I, the cations are disordered. In phase II, the cations are ordered and two successive cations along the **a** direction cannot be related by a translation of *a*/2 because the Cp* ligands have different orientations. The symmetry independent moieties of the asymmetric unit of phase II are colored differently. Disorder and the H-atoms are omitted for clarity

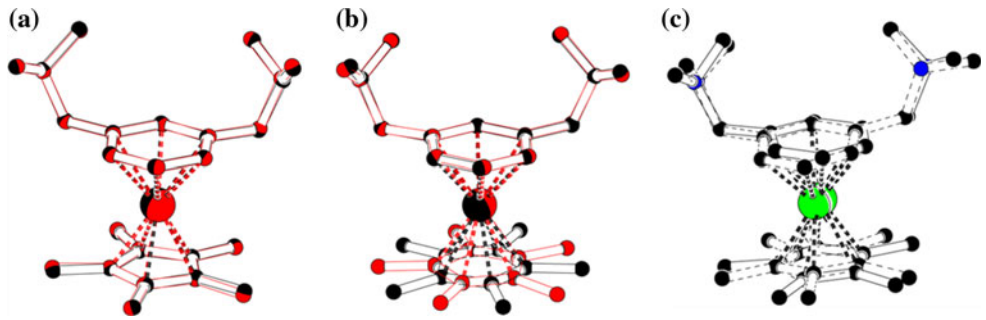

Fig. 6 **a** Quaternion fit of the two crystallographically independent cations 1 and 3 (or 2 and 4) for data collected at 150 K. The fitting transformation method suggests that these cations are related by a pseudoglide plane symmetry (see text). **b** Quaternion fit of the two crystallographically independent cations 1 and 2 (or 3 and 4) for data collected at 150 K. The fitting of these cations, which are related by a pseudotranslation of $a_{II}/2$ (see text), is only good for the $[Ru(\eta^6\text{-}1,3\text{-}(Me_2NCH_2)_2C_6H_4]^{2+}$ fragment. The difference in orientation of the Cp* ligands is clear. **c** Disordered cation $\mathbf{6}^+$ observed in phase I

and Ru13···Ru14 are found to be 8.3004 (10) and 8.1000 (10) Å, which are about 1% longer and 1.5% shorter than *a*/2 [i.e., 8.220 (<1) Å]. A *MolFit* for cations that are related by pseudotranslation suggested that those cations have similar conformations around the $Ru(\eta^6\text{-}1,3\text{-}(Me_2NCH_2)_2C_6H_4)$ parts but adopt different orientations for the Cp* ligands (Fig. 6b).

The four independent counter anions can be also related via pseudosymmetry. The rms deviations for fitting were always found to be less than 0.03 Å for both pseudo-glide plane and pseudo-translation symmetries.

Order–Disorder Transition

Measurements of the volume per formula unit *V*/*Z* versus *T* suggest that the cooling and heating transitions $T_{II \leftarrow I}$ and $T_{II \rightarrow I}$ are found near 213 and 217 K, respectively. The transition I ↔ II is characterized by a small $|\Delta V/Z|$ of about 3.14(10) $Å^3$, and the estimated width of hysteresis is 6(2) K. This solid–solid transition is likely to be first order because the *V*/*Z* versus *T* profile indicates a discontinuity and some hysteresis at the transition point [25]. Inspection of the diffraction pattern (Fig. S3) confirms that the crystal undergoes some structural changes in the *T*-ranges 212–215 K (cooling regimen) and 215–218 K (heating regimen), which is in good agreement with the measurements of the *V*/*Z* versus *T* profile.

The transition I ↔ II is of order–disorder type. The transition is associated by a change in Z': 1 ↔ 4, by the doubling of the *a* axis, and structural changes are driven along the **a** direction. The $Z' = 4$ structure (phase II) is an ordered modulated variant of the simpler, but disordered $Z' = 1$ structure (phase I). Disorder of the cations (in phase I) arises because the information (i.e., the information contained into the *h* odd reflections for phase II) about the different conformations of the independent cations along the **a** direction is lost as the thermal motion becomes large in the crystal lattice. Disorder of the cation may be approximated as being the superimposition of two adjacent cations (i.e., the cations 1 and 2 or the cations 3 and 4) found along the **a** direction of the structure of phase II (Fig. 6c). The spherical counter anions BF_4^- are found to be dynamically disordered at room temperature (i.e., the anions may have several energetically favorable orientations), which is not surprising since those anions do not take part in any strong interactions.

It is believed that the occurrence of this transition results from a significant change of thermal motion in the crystal as the temperature varies. Along the direction of greatest structural changes (i.e., the **a** direction), adjacent cations must acquire enough thermal motion so that their different conformations can be averaged in the room-temperature phase. Such an event may occur only if the arcs of oscillation around the normal of the best molecular planes of the Cp* ligands are large (Fig. S4).

$Z' > 1$

Structures with $Z' = 4$ are not common. A search of the November 2008 version (5.30+ updates through September 2009) of the Cambridge Structure Database (hereafter, CSD) [26] was made for structures having $Z' = 4$, three-dimensional coordinates determined, and $R < 0.10$. There were 1512 hits, which correspond to about 0.33% of the crystal structures archived in the CSD.

In the system $[\mathbf{6}](BF_4)$, the most favorable packing arrangement along the 2-D planes parallel to (0 0 1) is achieved when adjacent cations along the **a** direction have Cp* ligands approximately rotated by an angle of 36°, and when adjacent cations along the **b** direction have Cp* ligands with the same orientation (Fig. 7). This packing arrangement minimizes the amount of highly unfavorable contacts and void spaces in the crystal structure, but prevents a $Z' = 1$ structure to be ordered because adjacent

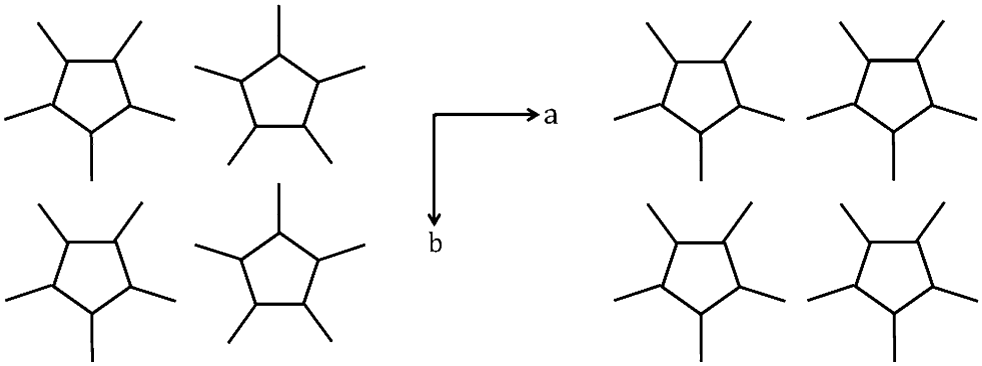

Fig. 7 Drawing showing a favorable (*left*) and unfavorable (*right*) packing for cations found in the 2-D planes parallel to (0 0 1). Only the Cp* ligands are shown for clarity

cations found along the **a** direction cannot be related by any symmetry operations. Implication of phenomena such as packing problems and pseudosymmetry in the existence of high Z' structures have been discussed in the literature [27, 28].

Conclusions

The two-phase system [**6**](BF_4) has one reversible solid–solid phase transition that takes place between 212 and 218 K. This study shows that the transition occurs without any significant loss of crystallinity. The room- and low-temperature phases are closely related since their packing arrangements are similar. In the room-temperature phase (*Pbca*, $Z' = 1$), the structure is disordered because the difference in conformation for the adjacent cations is no longer distinguishable along the **a** direction when the thermal motion becomes large in the crystal. In the low-temperature phase ($P2_1/c$, $Z' = 4$) the structure is ordered but some symmetry is lost. The system [**6**](BF_4) is an example for which an ordered high-Z' structure is more favorable than an ordered structure with $Z' = 1$.

Supplementary Materials

Crystallographic data for the structures reported in this paper have been deposited with the Cambridge Crystallographic Data Centre as supplementary publication nos. CCDC-676542 (phase I) and CCDC-676543 (phase II). Copies of available material can be obtained, free of charge, on application to the Director, CCDC, 12 Union Road, Cambridge CB2 1EZ, UK (fax: +44-1223-336033 or e-mail: data_request@ccdc.cam.ac.uk).

Acknowledgments We gratefully acknowledge the support of this research by Utrecht University and the NRSC-Catalysis program. This work was also supported in part (A.L.S.) by the Council for the Chemical Sciences of The Netherlands Organization for Scientific Research (CW-NWO).

References

1. Albrecht M, van Koten G (2001) Angew Chem Int Ed 40:3750
2. Albrecht M, van Koten G (1999) Adv Mat 11:171
3. Singleton JT (2003) Tetrahedron 59:1837
4. Bonnet S, Lutz M, Spek AL, van Koten G, Klein Gebbink RJM (2008) Organometallics 27:159
5. Siegler MA, Parkin S, Selegue JP, Brock CP (2008) Acta Cryst B 64:725
6. Sielger MA (2007) PhD Dissertation, University of Kentucky. http://lib.uky.edu/ETD/ukychem2007d00664/dissertationMASiegler.pdf
7. Bernstein J (2002) Polymorphism in molecular crystals. Oxford University Press, USA
8. Bendeif EE, Dahaoui S, François M, Benali-Cherif N, Lecomte C (2005) Acta Cryst B 61:700
9. Barnett SA, Broder CK, Shankland K, David WIF, Ibberson RM, Tocker DA (2006) Acta Cryst B 62:287
10. David WIF, Ibberson RM, Cox SFJ, Wood PT (2006) Acta Cryst B 62:953
11. Fagan PJ, Ward MD, Calabrese JC (1989) J Am Chem Soc 111:1698
12. Nonius (1999) COLLECT; Nonius BV, Delft, The Netherlands
13. Schreurs AMM (2005) PEAKREF. University of Utrecht, The Netherlands
14. Duisenberg AJM, Kroon-Batenburg LMJ, Schreurs AMM (2003) J Appl Cryst 36:220
15. Schreurs AMM, Xian X, Kroon-Batenburg LMJ (2010) J Appl Cryst 43:70
16. Beurskens PT, Beurskens G, de Gelder R, Garcia-Granda S, Gould RO, Israel R, Smits JMM (1999) The DIRDIF99 program system. Technical Report of the Crystallography Laboratory, University of Nijmegen, The Netherlands
17. Sheldrick GM (1986) SHELXS86. University of Göttingen, Germany
18. Sheldrick GM (2008) Acta Cryst A 64:112
19. Sheldrick GM (1999-2003) SADABS. University of Göttingen, Germany
20. Sheldrick GM (2003) TWINABS. University of Göttingen, Germany
21. Duisenberg AJM (1992) J Appl Cryst 25:92
22. Duisenberg AJM, Hooft RWW, Schreurs AMM, Kroon J (2000) J Appl Cryst 33:893
23. Mackay AL (1984) Acta Cryst A 40:165
24. Spek AL (2003) J Appl Cryst 36:7
25. Herbstein F (2006) Acta Cryst B 62:341
26. Allen FH (2002) Acta Cryst B 58:380
27. Desiraju GR (2007) CrystEngComm 9:91
28. Anderson KM, Steed JW (2007) CrystEngComm 9:328